

Multi-wavelength properties of short GRBs with extended emission observed by Swift

Author: Michela Maria Dinatolo^{1,2}

Maria Grazia Bernardini², Paolo D'Avanzo², Riccardo Brivio², Matteo Ferro²

¹Università degli Studi di Milano, Milan, Italy

²INAF-OABR

Abstract

We present a detailed study of the multi-wavelength properties of a sample of short GRBs with extended emission (EE) observed by Swift. The sample consists of 11 events, selected from the SBAT4 sample by D'Avanzo et al., [2], which was subsequently expanded to include events up to 2021, [3]. This sample contains short GRBs bright in terms of observed peak flux in the BAT energy band and with favorable observational conditions from ground for the determination of redshifts from Earth. The properties of the prompt emission (hardness ratio, spectral evolution), as well as the temporal behaviour of the X-ray afterglow phase are compared to the genuine short GRBs of the SBAT4 sample, and with a similarly selected complete sample of long Swift GRBs (BAT6), [5], with the aim of identifying unique features that distinguish the class of short GRBs with EE.

Prompt phase

Using the BAT data, we extracted the light curves binned according to a signal to noise ratio fixed to 3. We used these to distinguish two phases for each GRB: the initial pulse, IP, and the extended emission, EE. We extracted the spectra for both the phases and performed a spectral analysis comparing different models (simple power law, power law with an exponential cutoff). We studied the temporal evolution of the photon index, reported in Figure 1. Using the spectra obtained, we computed the hardness ratio:

$$HR = \frac{S(50 - 100 \text{ keV})}{S(25 - 50 \text{ keV})} \quad (1)$$

In Figure 2 we plot the HR vs duration for both the phases identified and for the GRBs of the BAT6 and SBAT4 sample. The IP lies in the same region than the short GRBs, while the EE in the one of long GRBs in terms of HR. However, the EE lasts longer than the average duration of the long one. A KS test confirmed that the distributions of the duration for the two populations are statistically different.

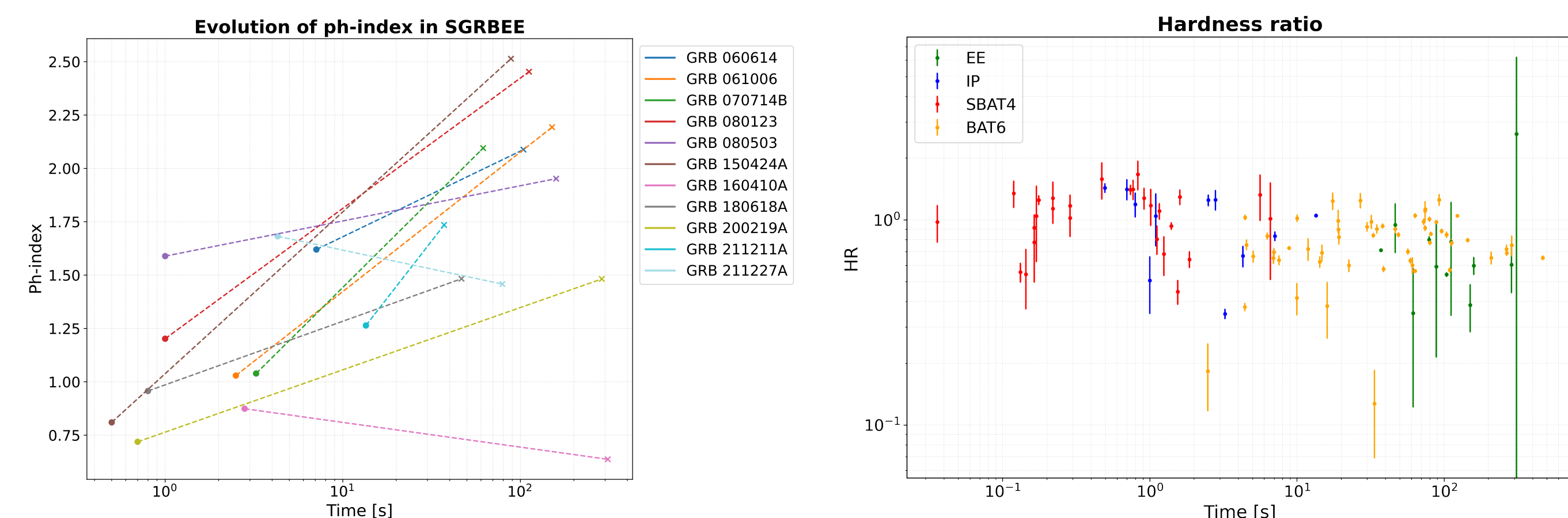


Figure 1. Ph -index of the SGRBEEs. The IP is indicated by a dot, the EE by a cross.

Figure 2. Hardness-duration plot for SGRBEEs (IP and EE) and for the samples SBAT4 and BAT6, see also [6].

E_{peak} - E_{iso} correlation

Three events from the sample were also detected by Fermi/GBM. We performed a spectral analysis using data from the two detectors with the best statistics. With the broader energy coverage provided by these observations, we were able to measure the rest-frame energies E_{peak} and E_{iso} for 2 IP and 1 EE. In order to compare a larger number of events with the BAT6 and SBAT4 samples, we used information from the Konus satellite and from literature, when available, see [7]. In Figure 3 we plot the E_{peak} - E_{iso} relation. The IP is always consistent with short GRBs, beyond the 3σ scatter, while EE lies in the same region identified for long GRBs.

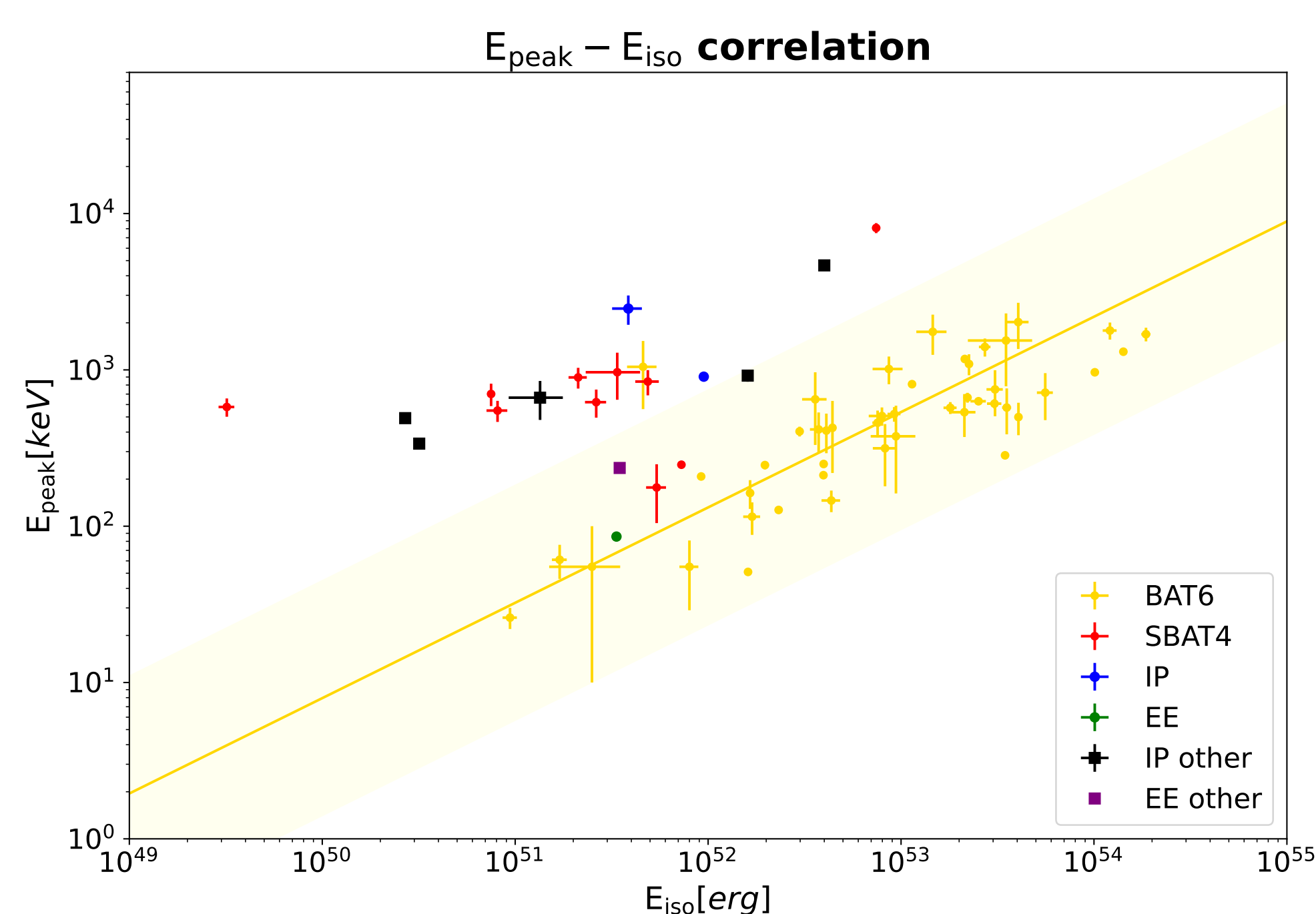


Figure 3. E_{peak} - E_{iso} relation, [1]. We reported in yellow the results for long GRBs of the BAT6 sample, with the power-law best fit is and the 3σ scatter of the distribution. We reported the information from Konus/Wind and the literature using black squares for the IP and purple for the EE. The green and blue dots refer to the GRBs observed by Fermi for which we performed the spectral analysis.

Conclusion

In this study, we performed a comprehensive characterization of SGRBEEs observed by Swift. The spectral properties and hardness of the IP are similar to those of short GRBs, while the EE resembles that of long GRBs. Considering the afterglow emission, GRBs with and without EE are indistinguishable at later times, while they differ at early times possibly due to the contribution of the EE in the X-ray energy band. We obtained the same result in the optical band. This sample can serve as a reference for all short GRBs with EE detected by other missions. It has already been used for GRB 240821A, observed by SVOM.

References

- [1] L. Amati et al. In: *AA* 390 (2002).
 [2] P. D'Avanzo et al. In: *MNRAS* 442 (2014).
 [3] M. Ferro et al. In: *AA* 678 (2023).
 [4] R. Margutti et al. In: *MNRAS* 428 (2012).
 [5] L. Nava et al. In: *MNRAS* 421 (2012).
 [6] D. A. Perley et al. In: *AJ* 696 (2009).
 [7] J.-P. Zhu et al. In: *AJL* 936 (2022).

Afterglow X

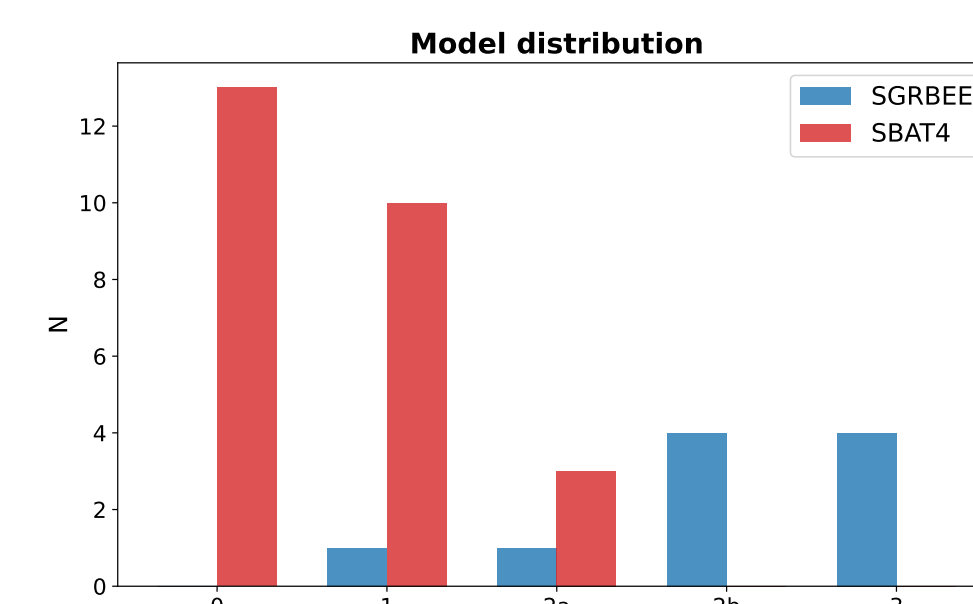


Figure 4. Distribution of the best model fit for short GRBs.

Figure 5 presents X-ray light curves observed with Swift/XRT, obtained from the Leicester database, in the common rest frame within the 2 – 10 keV energy band. GRBs with EE are indistinguishable from those without it in the SBAT4 sample, while they are fainter than for the BAT6 sample. We performed a morphological characterization of the light curves for both

populations, using the models described in [4]. In Figure 4, we present the distribution of the best-fitting models. GRBs with EE tend to display a more complex afterglow structure. Notably, none of the SBAT4 GRBs is best described by a type-3 model, which corresponds to light curves with three slope changes. To enable a direct comparison between the light curves of the two samples, we reconstructed them using the best-fitting model and evaluated their average evolution (see Figure 6). The two samples exhibit different light curve behavior only at early times both in flux and luminosity, within 400 s in the observer frame, while this discrepancy completely vanishes at later times and in the rest-frame representation. These findings are further supported by a KS test.

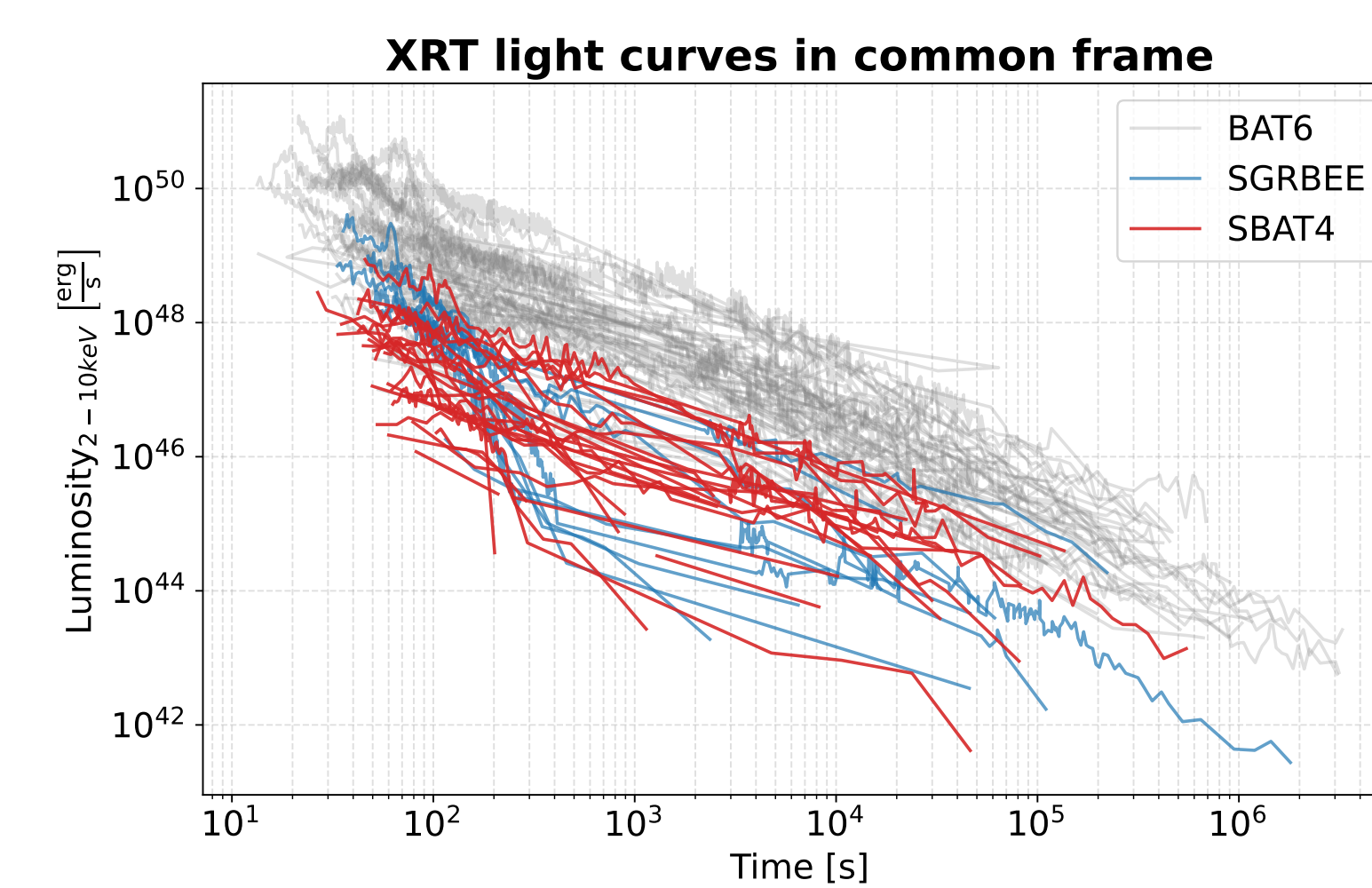


Figure 5. XRT light curves in common frame

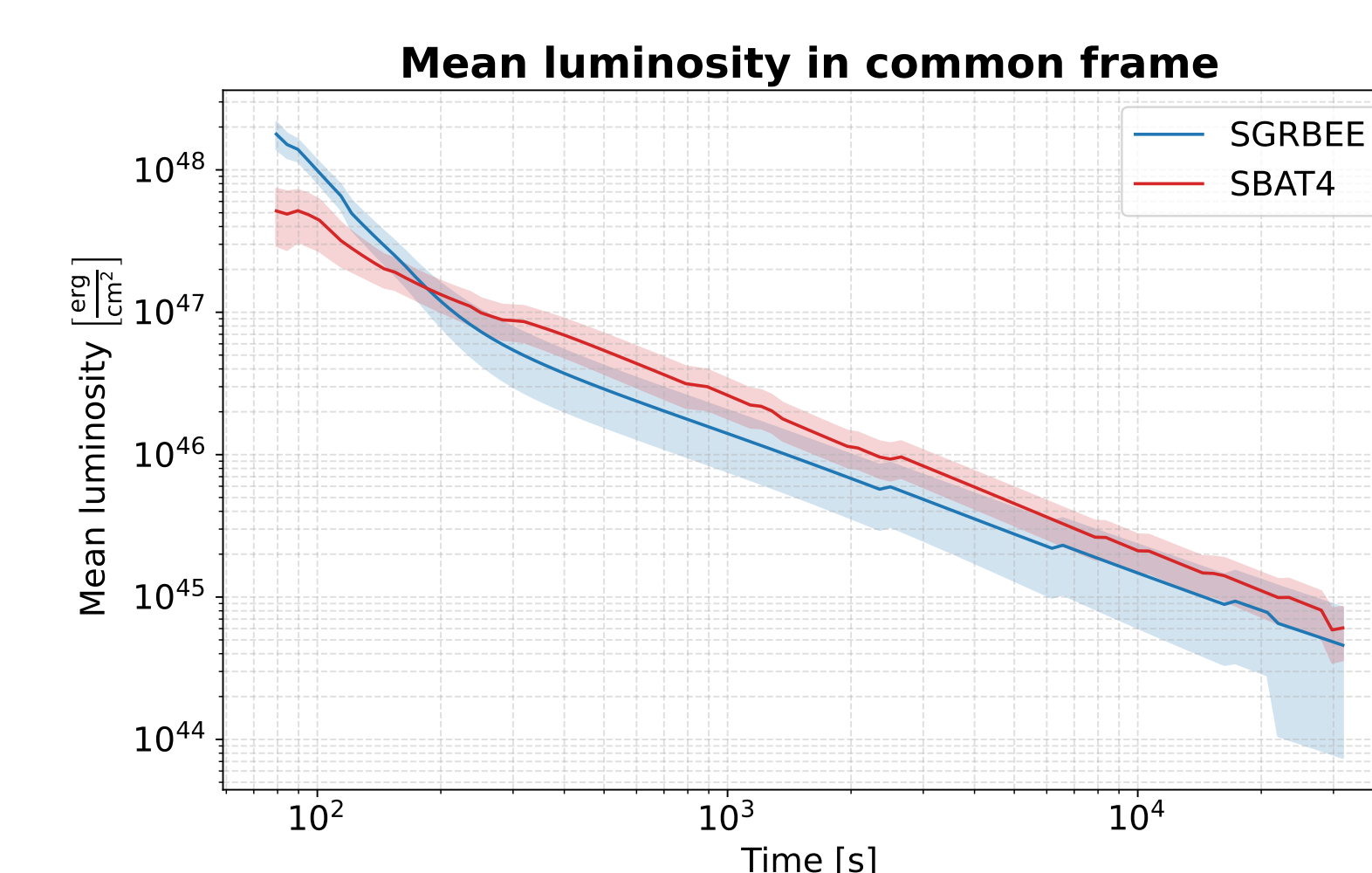
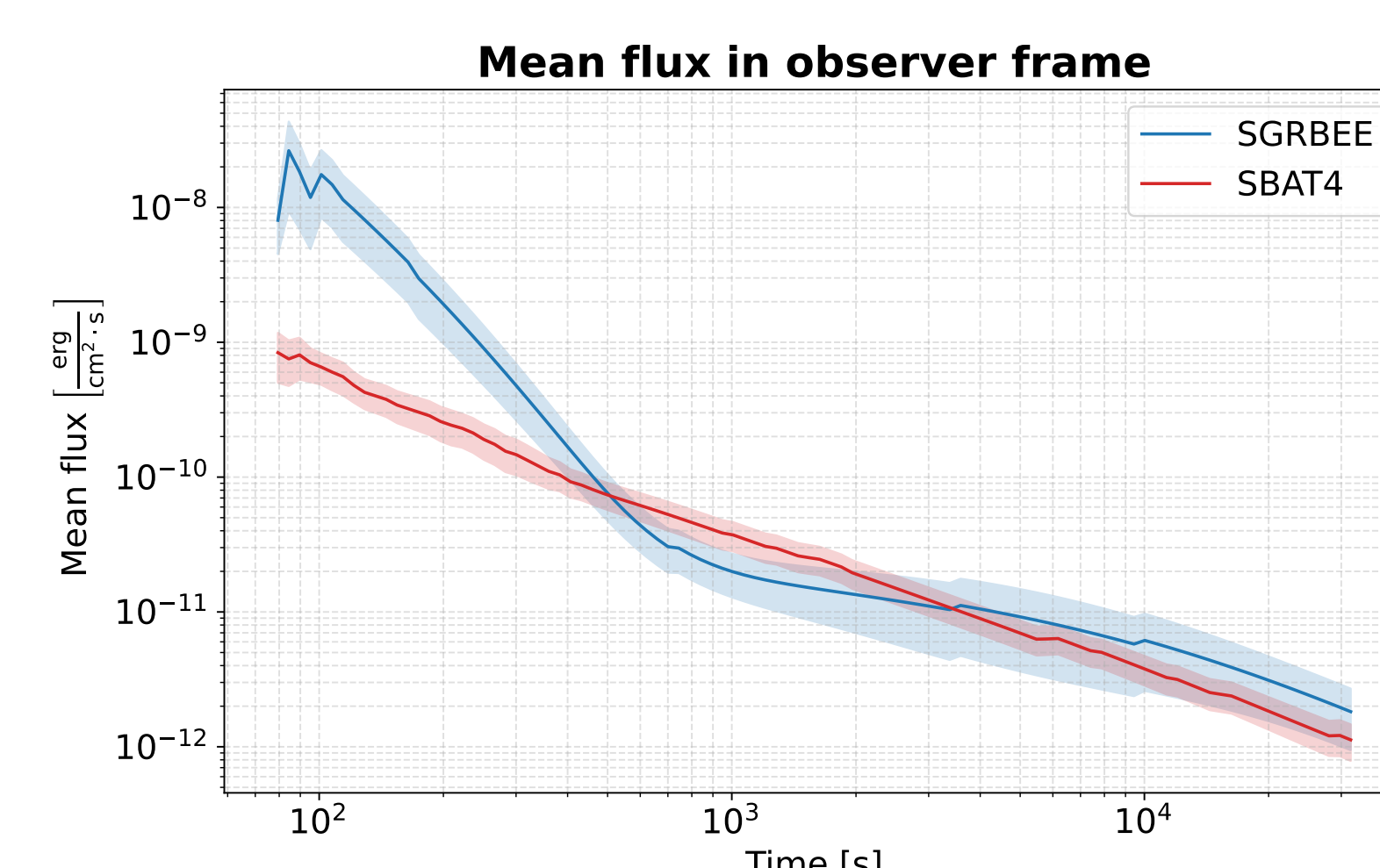


Figure 6. Mean value of the reconstructed light curves in observed frame (top) and common frame (bottom). The shaded area corresponds to the standard deviation of the distribution.